Article

Chinese Science Bulletin

Atmospheric Science

July 2012 Vol.57 No.19: 2460–2469
doi: 10.1007/s11434-012-5136-9

Distribution and origin of aerosol and its transform relationship with CCN derived from the spring multi-aircraft measurements of Beijing Cloud Experiment (BCE)

LU GuangXian[1,3] & GUO XueLiang[2*]

[1] *Laboratory of Cloud-Precipitation Physics and Severe Storms, Institute of Atmospheric Physics, Chinese Academy of Sciences, Beijing 100029, China;*
[2] *Chinese Academy of Meteorological Sciences, Beijing 100081, China;*
[3] *Graduate University of the Chinese Academy of Sciences, Beijing 100049, China*

Received February 3, 2012; accepted March 13, 2012; published online April 24, 2012

The atmospheric aerosol distribution, source and relationship with cloud condensation nuclei (CCN) observed during the Beijing Cloud Experiment (BCE) are analyzed. The results show that the high number concentrations of aerosol mainly distributed below 4500 m, and the magnitude could reach to 10^3 cm^{-3}. Above 4500 m, the aerosol number concentrations decreased to 10^1 cm^{-3} as the altitude increases, and the aerosol mean diameters were between 0.16 and 0.19 μm. Below 4500 m, the number size distributions of aerosol showed a bimodal (multimodal) mode, and an unimodal mode above it. Due to the different sources of aerosol, the conversion ratios of aerosol to CCN were less than 20% below 4500 m, and reached 50% above the level at 0.3% supersaturation. The back trajectories showed that aerosols at higher levels above 4500 m were strongly affected by large-size particles and those below 4500 m were strongly affected by local or regional pollution. Based on observations, a relationship between the CCN number concentration and aerosol number concentration is established.

aerosol, CCN, aircraft observation, number size distribution

Citation: Lu G X, Guo X L. Distribution and origin of aerosol and its transform relationship with CCN derived from the spring multi-aircraft measurements of Beijing Cloud Experiment (BCE). Chin Sci Bull, 2012, 57: 2460–2469, doi: 10.1007/s11434-012-5136-9

Aerosols are important trace component in the atmosphere and much attention have been paid to their effects on cloud and precipitation as well as climate system. On one hand, aerosols can directly absorb, scatter and reflect radiation, and change the radiation flux to the earth surface, which is referred to as direct effect. On the other hand, some aerosols may act as cloud condensation nuclei (CCN) or ice nuclei (IN) to involve in the formation of clouds, and change the microphysical and radiation properties of clouds, and then influence the climate system, which is referred to as indirect effect. The indirect effect can be further classified as first indirect effect or the Twomey effect [1] and second indirect effect or the Albrecht effect [2]. The Twomey effect refers that for given liquid water content, the increase of aerosol concentration will lead to an increase of cloud droplet concentration but a smaller effective diameter of cloud, and then result in an increase of albedo of clouds, while the Albrecht effect is that the increased aerosols can lead to smaller droplet diameter and inhibits the growth of cloud droplets and the formation of precipitation, thereby increases cloud lifetime.

Aerosols influence the climate system mainly through CCN and affect the microphysics of clouds. CCN is closely related to the chemical composition of aerosols. The chemical composition of aerosols, however, change greatly with spatial and temporal distributions, which causes the very difficult quantification of the aerosol indirect effect and brings large uncertainty on the study of cloud-aerosol interaction as well as the influence on the climate system. The IPCC report [3] pointed out that the aerosol indirect effect

*Corresponding author (email: guoxl@mail.iap.ac.cn)

lays the largest uncertainty on radiation forcing research. This uncertainty is mainly due to the lack of knowledge about aerosol spatial and temporal distribution, chemical composition and nucleation property. Thus observation and research of aerosol and CCN is significant.

Many international observational programs had been made against aerosol-CCN-cloud interactions, such as the Atlantic Stratocumulus Transition Experiment (ASTEX) [4], the Small Cumulus Microphysics Study (SCMS) [5] off the east coast of Florida, the Indian Ocean Experiment (INDOEX) [6], the Aerosol Characterization Experiment 1, 2 and 3 (ACE-1, 2, 3) [7–10], and the Cirrus Regional Study of Tropical Anvils and Cirrus Layers-Florida Area Cirrus Experiment (CRYSTAL-FACE) [11] in the vicinity of southwest Florida. These observational experiments provided large quantity of valuable data for aerosol-cloud interactions studies.

Chinese researchers have conducted numerous surface and aircraft observations of aerosol and CCN in the Helan Mountain area since 1990s and revealed the relationship between aerosol and CCN in different conditions in this area [12–16]. Zhang et al. [17] analyzed the aircraft observations of aerosol over Beijing and surrounding area in summer and autumn in 2003, and showed that aerosol number size distributions were greatly different in different weather conditions: the number size distribution was unimodal under 0°C level, and bimodal above. Fan et al. [18] analyzed the aircraft observations over the same area in August and September 2004, and suggested that aerosol number concentration was largest in cloudy day and smallest in clear day, the number size distribution was unimodal. Moreover, there was a distinct aerosol accumulation area under the inversion layers. Shi et al. [19] used surface and aircraft observations in Shijiazhuang in the autumn of 2005 and the spring of 2006 to study the spatial and temporal changes of CCN in the North China Plain. Duan et al. [20] analyzed the precipitation and visibility data from 1990 to 2005 in the North China Plain, and found that the anthropogenic aerosol suppressed precipitation in this area in summer. Zhang et al. [21] found that aerosol vertical distributions were strongly affected by weather and meteorological conditions, and they summarized three different types of aerosol vertical distributions corresponding to different weather systems. Moreover, Zhang et al. [22] analyzed aircraft observations in July 2008 and proved that high aerosol number concentration corresponded to the high cloud droplet number concentration and smaller diameter, and *vice versa*.

Since most observations were conducted during weather modification experiments or ground-based site [23–33], there are larger limitations to study aerosol-cloud interactions. Observational experiments designed specifically for aerosol-cloud interactions are still needed.

The Beijing Cloud Experiment (BCE) of the Key Project in the National Science & Technology Pillar Program during the Eleventh Five-year Plan Period was conducted from April to May in 2009 in Zhangjiakou area, which locates in upstream area of Beijing City. It is the first multi-aircraft cloud observational experiment in China. During this experiment, three aircrafts observed aerosol, CCN and cloud at different altitudes simultaneously, and provided valuable data for the aerosol-cloud interactions in this area. This study intents to analyze the data of 18 April, 30 April and 1 May from this experiment to reveal the properties of aerosol and CCN, and their relationship.

1 Instruments and experiment

The BEC was conducted in April and May 2009 and the observational area is located in the north of Zhangjiakou city (shown in the box of Figure 1). Three aircrafts took off from airports in Zhangjiakou, Shijiazhuang and Taiyuan respectively, and made observations at different altitudes simultaneously in the study area.

The aircrafts used in this experiment were the Cheyenne III-A from the Shijiazhuang Weather Modification Office, the Beijing Y-12 from the Beijing Weather Modification Office and the Datong Y-12 from the Shanxi Weather Modification Office. Instruments carried on aircrafts were:

Shijiazhuang Cheyenne III-A: Forward Scattering Spectrometer Probe extended range (FSSP-ER), Passive Cavity Aerosol Spectrometer Probe model 100X (PCASP-100X), 2D-Gray cloud probe (OAP-2D-GA2), 2D-Gray precipitation probe (OAP-2D-GB2), Cloud Condensation Nuclei Counter (CCNC) and Hot Wire Liquid Water Probe (King-LWC).

Beijing Y-12: Cloud Aerosol and Precipitation Spectrometer (CAPS, including the Cloud and Aerosol Spectrometer (CAS), the Cloud Imaging Probe (CIP) and the Liquid Water Content Sensor (LWC-100)), Precipitation Imaging Probe (PIP), PCASP-100X with SPP-200 module (SPP-200), Cloud Condensation Nuclei Counter (CCNC)

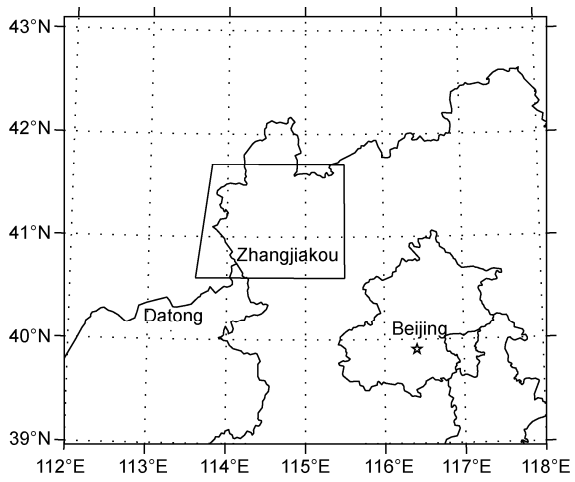

Figure 1 Observational area.

and Aircraft Integrated Meteorological Measurement System (AIMMS-20).

Datong Y-12: Cloud Droplet Probe (CDP), Cloud Imaging Probe (CIP), Precipitation Imaging Probe (PIP), Cloud Condensation Nuclei Counter (CCNC), Aircraft Integrated Meteorological Measurement System (AIMMS-20) and Hot Wire Liquid Water Probe (LWC-100).

Table 1 lists the instruments used in the BCE. Aerosol data were collected with the SPP-200 (Droplet Measuring Technologies, DMT) on aircraft of the Beijing Y-12 and the PCASP-100X (Particle Measurement System, PMS) on aircraft of the Shijiazhuang Cheyenne III-A. The Datong Y-12 aircraft had no aerosol particle probe. The Spp-200 measures aerosol number size distribution with diameter from 0.1 to 3.0 μm, which is divided into 30 bins and the resolution changes with particle size. The PCASP-100 is the same with the SPP-200 but it is divided into 15 bins. All of these two probes sample 1 data per second. CCN number concentrations were measured using the CCN Counter (DMT) on the three aircrafts. The CCN Counter can operate at supersaturation (S) from 0.1% to 2.0%. It can be set to single or as much as five different S to observe continuously with a sample rate of 1 Hz. The CCN Counter was operated at a single supersaturation of 0.3% during the BCE. The inlet was mounted on the top of aircrafts and connected to a stainless steel tube. In this experiment, the pressure in the CCN Counter chamber was equal to the environmental pressure because there was no inlet pressure controller to control the sample flow.

All instruments were calibrated by the DMT in America before the experiment started, moreover, the PCASP, SPP-200 and CAPS were calibrated using polystyrene latex spheres every month. The CCN Counters were calibrated with monodisperse ammonium sulphate or sodium chloride particles, and see Rose et al. [34] for detailed description.

Three observations were conducted on 18 April, 30 April and 1 May in 2009 respectively. Data from the Datong Y-12 will not be analyzed in this study due to no aerosol data. Table 2 lists the observation times of the Shijiazhuang Cheyenne III-A and Beijing Y-12.

The aircrafts Observed at different levels when all of them flew into the observational area. Figure 2 shows observational altitudes of Beijing Y-12 and Shijiazhuang Cheyenne III-A when they were in the observational area during the experiment. The Beijing Y-12 flew mainly at 3600 and 3700 m, and sometimes observed at cloud base, such as 2700 m on 18 April and 2400 m on 30 April. The Shijiazhuang Cheyenne III-A observed mainly at 4800, 5600 and 6000 m.

During the observation on 18 April, the Zhangjiakou region was at the south edge of a low pressure weather system and the surface was dominated by south-west wind. The corresponding 700 hPa and 500 hPa levels were controlled by a weak westerly trough. Figure 3 is infrared cloud images from satellite FY 2-C during the BCE. Figure 3(a) shows that the cloud was located in the north of Zhangjiakou region, and the cloud in the observational area was thin. A cold front passed over the Zhangjiakou region between 20:00 LT on 30 April and 08:00 LT on 1 May, and 5.3 mm precipitation was recorded by the Zhangjiakou Meteorological Observation. At 20:00 30 April, the front had arrived at the marches with Hebei, Shanxi and Inner Mongolia, and the observational area was located in front of the frontal weather system. The edge of the cloud system had covered the observational area and the main body of the cloud system was located in the west of this area (Figure 3(b)). The frontal weather system had moved to the east of Hebei Province at 08:00 on 1 May and the observational area was located behind the frontal system. Figure 3(c) shows that the cloud had moved out of the observational area. The upper

Table 1 Instruments used in the BCE

Instrument	Variable	Size range	Resolution
FSSP-ER	cloud particles	15 bins, 4 measurement ranges: 5–95 μm, 2–47 μm, 2–32 μm and 1–16 μm	measures in 4 size ranges, used the range of 2–47 μm, resolution is 3 μm
PCASP-100X	aerosol particles	15 bins, 0.1–3 μm	from 0.02 to 0.5 μm
OAP-2D-GA2	cloud particles, precipitation particles	62 bins, 25–1550 μm	25 μm
OAP-2D-GB2	precipitations	62 bins, 100–6200 μm	100 μm
CCN Counter	CCN concentration	particle size range: 0.75–10 μm supersaturation range: 0.07%–2.0%	about 30 s for 0.2% supersaturation change
King-LWC	liquid water content	0–3 g/m^3	–
CAS	aerosol particles and cloud particles	30 bins, 0.6–50 μm	Changes with the particles size
CIP	cloud particles, precipitation particles	62 bins, 25–1550 μm	25 μm
PIP	precipitation particles	62 bins, 100–6200 μm	100 μm
SPP-200	aerosol particles	30 bins, 0.1–3 μm	changes with the particles size
CDP	cloud particles	30 bins, 2–50 μm	changes with the particles size
AIMMS-20	meteorological parameters	–	–

Table 2 Observation times during the BCE

	Shijiazhuang Cheyenne III-A	Beijing Y-12
18 April	17:00–18:12	17:05–18:55
30 April	18:26–19:30	17:30–19:24
1 May	09:11–10:30	08:31–11:34

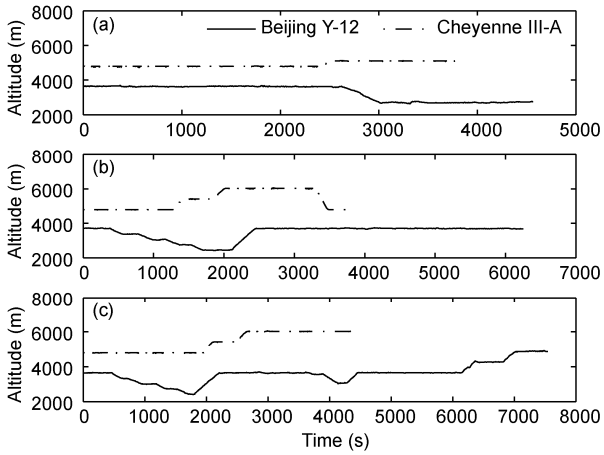

Figure 2 Observation altitude of Beijing Y-12 and Shijiazhuang Cheyenne III-A during BCE. (a) 18 April; (b) 30 April; (c) 1 May.

levels over observational area were controlled by a westerly trough during the passing of the cold frontal weather system, thus, the weather process from 30 April to 1 May was produced by the combined action of surface cold frontal weather system and westerly trough.

2 Results

The clouds can greatly affect the results of CCN observation. To obtain the relationship between aerosol and CCN, we must minimize the effects of clouds by excluding the data that contaminated by clouds. The first step is to distinguish the in-cloud and out-of-cloud data from the overall dataset. In fact, there is no generally acknowledged criterion to determine the appearance of clouds from the data, so that scientists use their own criterions in their researches [22,35–39]. In addition, there is no comparison study to evaluate influences of using different criterions. Refer to works of Hobbs et al. [37] and Zhang et al. [22], the following criterion is used to determine the appearance of clouds in this study: the concentration of droplets with diameters between 3 and 5 μm is $\geqslant 10$ cm^{-3} (as measured by the FSSP-ER or the CAS), or the concentration of droplets with diameter larger than 100 μm is $\geqslant 0.1$ cm^{-3} (as measured by the CIP or the OAP-2D).

2.1 Vertical distributions of aerosol number concentration, diameter and size distribution

We can get the aerosol vertical distribution in the observational area by using multi-aircrafts to observe at different levels. Statistical properties of out-of-cloud aerosols and CCN at different levels during the experiment are listed in Table 3, the aerosol number concentration (N_a), mean diameter (MD), relative dispersion (ε), CCN number concentration (N_{ccn}) and the ratio of CCN number concentration to aerosol number concentration (N_{ccn}/N_a) are listed in columns 3 to 8 respectively. Data that collected by the Beijing Y-12 at the level of 4800 m on 1 May will not be analyzed since the flight at this level was all located in the cloud.

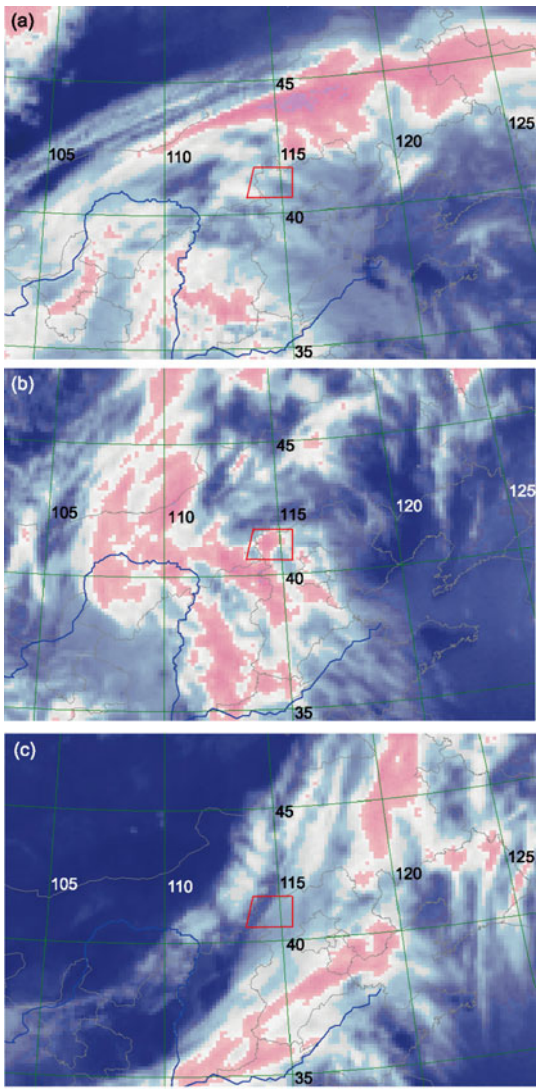

Figure 3 FY 2-C infrared cloud images during BCE. (a) 18:00 on 18 April; (b) 18:00 on 30 April; (c) 09:00 on 1 May. Red box shows the observed.

Figure 4 shows the vertical distributions of aerosol number concentration, mean diameter and relative dispersion. Data in this figure came from Table 3. Observation under 3700 m was made by the Beijing Y-12, and that above it was made by the Cheyenne III-A except for observations at 4200 m and at 4800 m on 1 May, which were made by the Beijing Y-12.

Under the influence of surface pollutants, high aerosol

Table 3 Statistical properties of aerosols and CCN at different levels during the BCE [a)]

Date	Aircrafts	Altitude (m)	N_a (cm^{-3})	MD (μm)	ε (Relative dispersion)	N_{ccn} (cm^{-3})	N_{ccn}/N_a
2009-04-18	Beijing Y-12	2700	6534	0.19	0.39	985	0.151
	Cheyenne III-A	3600	2796	0.18	0.43	346	0.124
		4800	369	0.18	0.53	78	0.211
		5100	183	0.17	0.48	52	0.284
2009-04-30	Beijing Y-12	2400	3194	0.18	0.53	475	0.149
	Cheyenne III-A	3700	2471	0.18	0.57	300	0.121
		4800	87	0.16	0.48	26	0.299
		5400	51	0.16	0.46	23	0.451
		6000	33	0.17	0.49	16	0.485
2009-05-01	Beijing Y-12	3600	2068	0.12	0.49	34	0.016
		4200	2419	0.11	0.51	34	0.014
		4800	–	–	–	–	–
	Cheyenne III-A	4800	73	0.22	0.89	10	0.137
		5400	31	0.17	0.55	6	0.194
		6000	52	0.17	0.59	20	0.385

a) CCN was observed at the supersaturation of 0.3%.

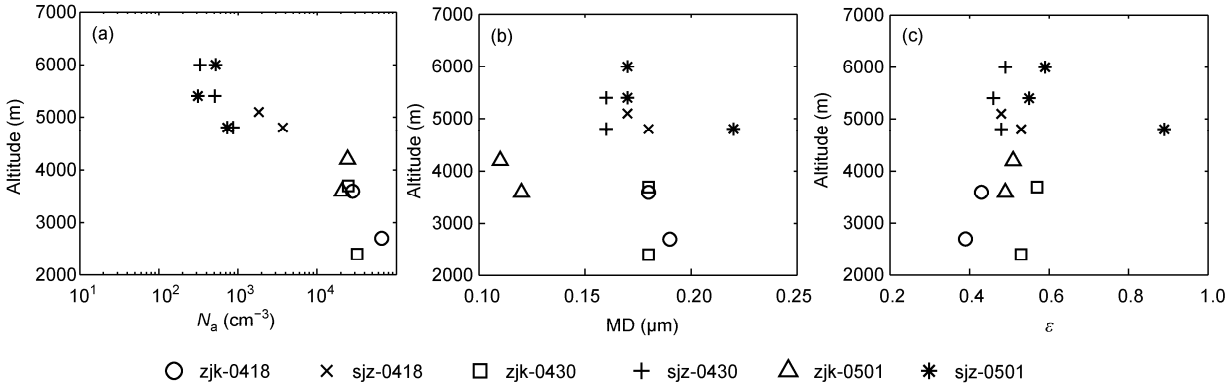

Figure 4 Vertical distributions of aerosol (a) number concentration N_a; (b) mean diameter MD; (c) relative dispersion ε. In the legend, zjk and sjz represent the Beijing Y-12 aircraft and Cheyenne III-A aircraft, respectively. The numbers behind represent the date, such as 0418 means 18 April.

number concentrations appeared at lower levels (Figure 4(a)), the highest value was 6534 cm^{-3} at 2700 m on 18 April. Atmosphere was in stable stratification during the BCE, and the convective transport was weak, so that the airflow lifting and turbulence diffusion were the major mechanisms of vertical transport of aerosols, which made hard to transport the pollution aerosol to upper levels of the atmosphere. For this reason, the aerosol number concentration generally decreased as altitude increased: high number concentrations of aerosol were mainly distributed in the levels under 4500 m, and decreased to less than 100 cm^{-3} in the levels above it.

Except for the observations on 1 May, the aerosol mean diameter was about 0.16–0.19 μm (Figure 4(b)), and varied little with altitude. This was consistent with observations from 2005 to 2006 in Beijing [21]. On 1 May, the mean diameter was 0.12 μm and 0.11 μm at 3600 m and 4200 m respectively, much smaller than other two days observations. This suggests that larger aerosols were depleted by clouds during the passing of the cold frontal system. The corresponding aerosol number concentrations changed little, and were 2068 and 2419 cm^{-3} respectively. We can rule out the effect from clouds, because the data that contaminated by clouds have been excluded during data pre-procession. There were two reasons that might lead to the phenomenon of high aerosol concentration with small diameter. (1) The advection. Observations on 1 May were made in the morning after the front passed, and local aerosols could hardly be transported to these levels, so, these small aerosols might be advected from outside area by the cold air accompanied with the frontal weather system. (2) The secondary aerosol. Peter et al. [40] studied a case with pre-frontal and post-frontal aircraft observations during the ACE-Asia, and suggested that mixing between air masses with large gradients in temperature and relative humidity might have promoted new particle formation. Moreover, the evaporation of cloud droplets behind the frontal cloud system was an important source of aerosol. In contrast with mean diameters under

4500 m, mean diameters were larger at those above it, especially at 4800 m (0.22 μm).

The relative dispersion (ε), defined as the quotient of the standard deviation about mean diameter (σ) dividing the mean diameter itself, and describes the relative width of aerosol size spectra. Figure 4(c) shows the change of ε of average aerosol size spectra with altitude during the BCE. Values of ε changed mainly from 0.4 to 0.6 with altitude in the same day, and suggested that the aerosol size spectra changed little with altitude. Although aerosol mean diameters were much smaller than those in other two days at 3600 m and 4200 m on 1 May, values of ε were much the same. However, values of ε on 1 May were much larger than those in the other two days in the area above 4500 m, especially at 4800 m, it reached as large as 0.89, and suggested that aerosol size spectra were wider in the area above 4500 m than in below.

Figure 5 shows the aerosol average number size distributions at different levels. The spectral patterns below 4500 m were different greatly from those above. At lower levels, aerosol spectra were dominated by high concentration of small particles (Figure 5(a)), and showed a bimodal distribution with peak diameters at 0.1 and 0.14 μm respectively. On 18 April, a peak diameter even appeared between 0.2 and 0.24 μm. However, aerosol spectra showed unimodal distribution above 4500 m with peak diameter at 0.1 μm. Spectral patterns of 18 and 30 April were much the same but total concentrations of 18 April were higher.

Aerosol spectra of 1 May were different greatly from that of 18 and 30 April. Firstly, small particles increased greatly at 3650 and 4270 m. Aerosol concentrations of the smallest bin (0.1 μm) at these levels increased to 37660 cm^{-3} and 44380 cm^{-3} on 1 May, and the largest value in the other two days was 15650 cm^{-3}. Secondly, concentrations of aerosols with diameter ranging from 0.12 to 3 μm, especially from 0.16 to 0.3 μm, decreased distinctly. For example, the concentration of aerosol with diameter of 0.22 μm at 3600 m on 18 April was 6517 cm^{-3}, and decreased to 392 cm^{-3} on 1 May because of the depletion of large particles by cloud and precipitation when the front passed. Comparing with 30 April, the concentrations of aerosols with diameter ranging from 1.8 to 3 μm at 4270 m on 1 May increased, a peak diameter even appeared at 2.4 μm with concentration of 4.8 cm^{-3}. Moreover, at levels above 4500 m, the concentrations of aerosols with diameter larger than 0.6 μm on 1 May were higher than that on 30 April, and a second peak appeared at 2.4 μm with concentration of 5.4 cm^{-3}. These phenomena were in good agreement with results in Figure 4.

2.2 Vertical distribution of cloud condensation nuclei (CCN) and its relationship with aerosol

Cloud condensation nuclei (CCN) are critical to cloud formation and its microphysical properties. The CCN concentrations at different levels were measured with CCN Counters (CCNC) that carried by the aircrafts, and the supersaturation of 0.3% was set during the whole experiment.

Figure 6 shows the vertical distribution of CCN concentration (N_{CCN}) at 0.3% supersaturation and the ratio of CCN concentration to aerosol number concentration. The CCN concentrations decreased as altitude increased (Figure 6(a)). On 1 May CCN concentrations were much lower than those in the other two days because of the depletion of CCN when the front passed. At about 3600 m, the CCN concentration was 300 cm^{-3} on 30 April, and decreased to 34 cm^{-3} on 1 May. Also, the CCN concentration decreased from 23 cm^{-3}

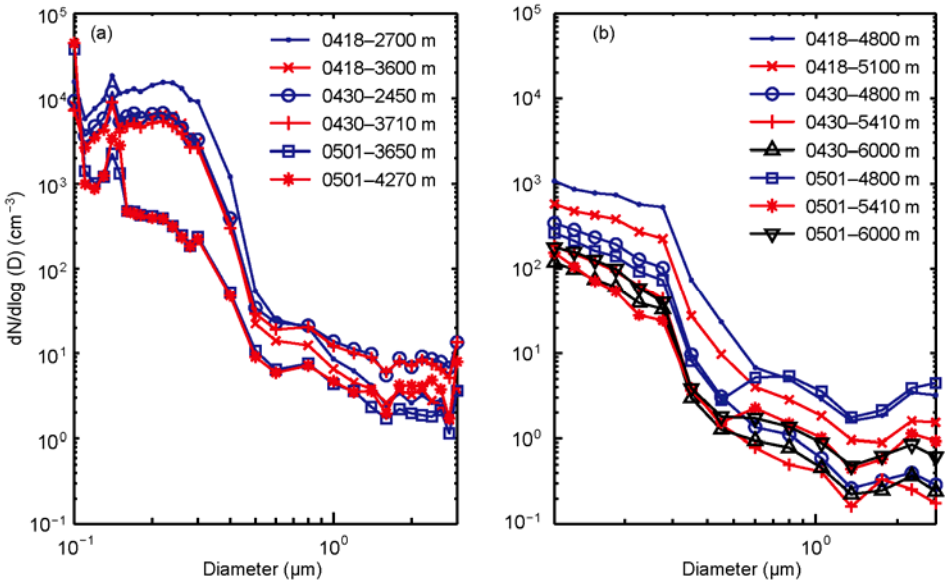

Figure 5 Average aerosol number size distributions at different levels. (a) Levels below 4500 m (observed by Beijing Y-12); (b) levels above 4500 m (observed by Cheyenne III-A). In the legend, the first four numbers represent the observe date and the numbers behind represent the observational levels.

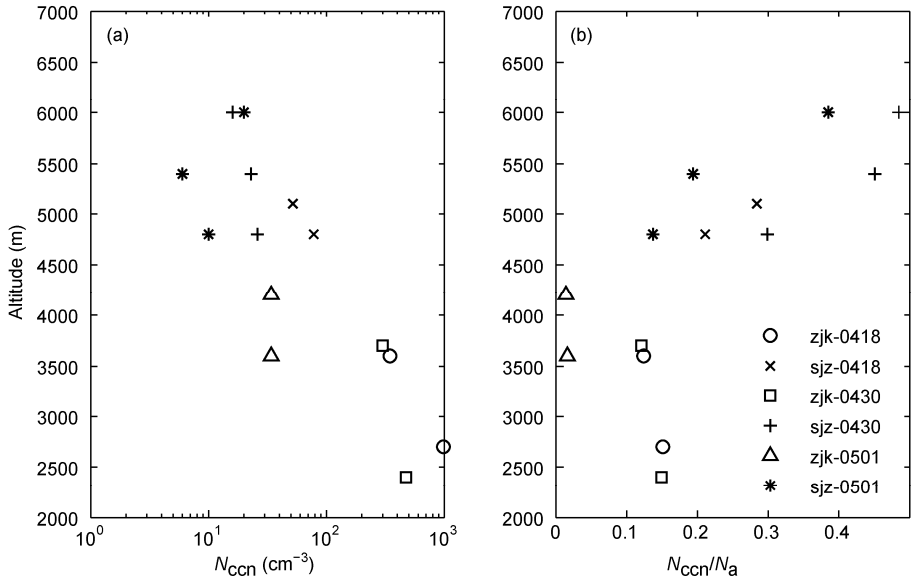

Figure 6 Vertical distributions of (a) CCN concentration; (b) ratio of CCN concentration to aerosol number concentration at 0.3% supersaturation. Legend is the same as in Figure 4.

on 30 April to 6 cm^{-3} on 1 May at 5400 m. In addition, we can also find from Figure 6(a) that the CCN concentration at 6000 m increased on 1 May compared with that on 30 April.

The ratio of CCN concentration to aerosol number concentration can be used to represent the rate that aerosols transform into CCN at a certain supersaturation. Figure 6(b) shows that ratios were smaller than 0.2 at levels below 4500 m, it means that less than 20% of aerosols could act as CCN at supersaturation of 0.3%. Ratios ranged from 0.122 to 0.15 on 18 and 30 April, and then decreased to the range from 0.014 to 0.016 on 1 May, which were much less than those in the other two days. At levels above 4500 m, ratios increased with altitude, and ranged from 0.2 to 0.5. For example, ratios increased from 0.299 and 0.137 at 4800 m to 0.485 and 0.385 at 6000 m on 30 April and 1 May respectively. It means that at the supersaturation of 0.3%, the proportion of aerosols that could act as CCN increased with altitude and could reach as large as 50% at 6000 m. The ability of aerosol to act as CCN depends on its size and chemical composition. For particles with similar chemical composition, the larger the particles, the easier they can be activated. Therefore, Figure 6(b) suggests that at lower levels of the atmosphere over the observational area, the particles were too small to act as CCN; at upper levels, the larger soluble particles were much easier to be activated. Differences of aerosol properties in altitude shown in Figures 4–6 indicate that aerosol sources and properties were different in the upper and lower atmosphere.

The measurement of CCN concentration is more difficult than aerosol, we hope to use the aerosol number concentration to represents the CCN concentration, so that the determination of the relationship between aerosol number concentration and CCN concentration is critical. The CCN activating property is complicated [32,34,41], mainly depends on particle size and chemical composition. With the experimental data, we hope to find a simple relationship between CCN and aerosol number concentration at a certain supersaturation without the chemical composition information. Figure 7 shows the relationship between average aerosol number concentration and CCN concentration at different levels, and the dash and solid lines are fittings including (fit1) and excluding (fit2) observation on 1 May. The correlation coefficients of fit1 and fit2 were 0.84 and 0.98 respectively, and it suggests that the fitting result without observations on 1 May was better than that with them. Moreover, the observations below 4500 m on 1 May influenced the fitting result much stronger than that above. One of the reasons is that the large quantity of aerosols was scavenged by cloud and precipitation when the front passed.

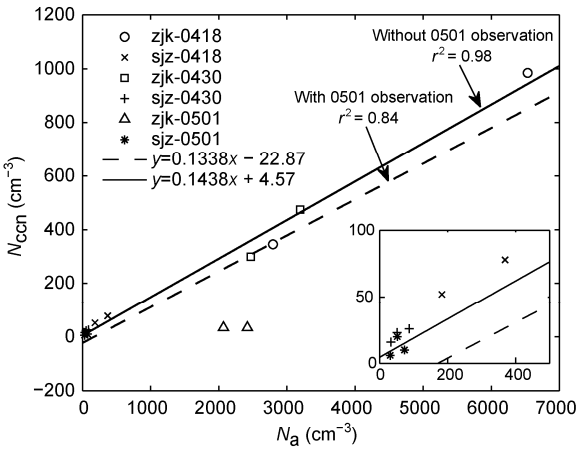

Figure 7 Relationship between aerosol and CCN concentration. Dash and solid lines are fittings include and exclude observations on 1 May.

2.3 Aerosol sources and properties

Vertical distributions of aerosol number concentration, mean diameter and size distribution suggested that there were large differences between the lower (under 4500 m) and upper (above 4500 m) atmosphere, which resulted in differences of conversion ratios of aerosol to CCN between different levels. In order to understand the sources and properties of aerosols at different levels during the experiment, we performed 48-h back trajectory analyses based on the National Oceanic and Atmospheric Administration (NOAA) Hybrid Single-Particle Lagrangian Integrated Trajectory (HYSPLIT) model.

Figure 8 shows the 48-h back trajectories of air masses during the experiment. The black stars represent the observational area; lines of different colors represent different back trajectories at different levels, and the time in the figures is UTC. Back trajectories revealed the different sources and transport paths of air masses sampled in these three days. The air mass sampled on 18 April was originated from the Inner Mongolia and moved slowly, and it took 48 h to reach the observational site. Since the air mass was primarily formed by low-level lifting process, the effect of local pollution was much larger during the moving of air mass (Figure 8(a)). All of these result in the high concentrations of aerosol and CCN at different levels. Figure 8(b) shows that the air mass sampled on 30 April was originated from Xinjiang area. It passed through the Gobi Desert, and entered Shaanxi and Shanxi provinces, and subsequently moved slowly into the observational area. Comparing with 18 April, the air mass on 30 April was less influenced by surface pollutants since the aerosol concentrations at lower levels were smaller. Air mass sampled on 1 May was originated form Taklimakan Desert area and Kyrgyzstan, which are important dust sources (Figure 8(c)). The high moving speed made it have less influence by local environment, and the appearance of dust at higher levels made the concentration of particles with diameter ranging from 0.6 to 3 μm much higher than the other two days.

The back trajectories suggested that levels above 4500 m were influenced by large particles in these three days during the experiment. The high CCN to aerosol ratio (as large as 50%) suggested the high solubility of these large particles, and it had greater effect on cloud and precipitation under stable weather condition. The levels below 4500 m were influenced more by local and surface pollutants, and the conversion ratio of aerosol to CCN was as low as 20% although the pollution aerosol concentration was high. Under a stable weather condition, these pollution aerosols had less effect on cloud and precipitation because it was difficult to transport them to upper levels.

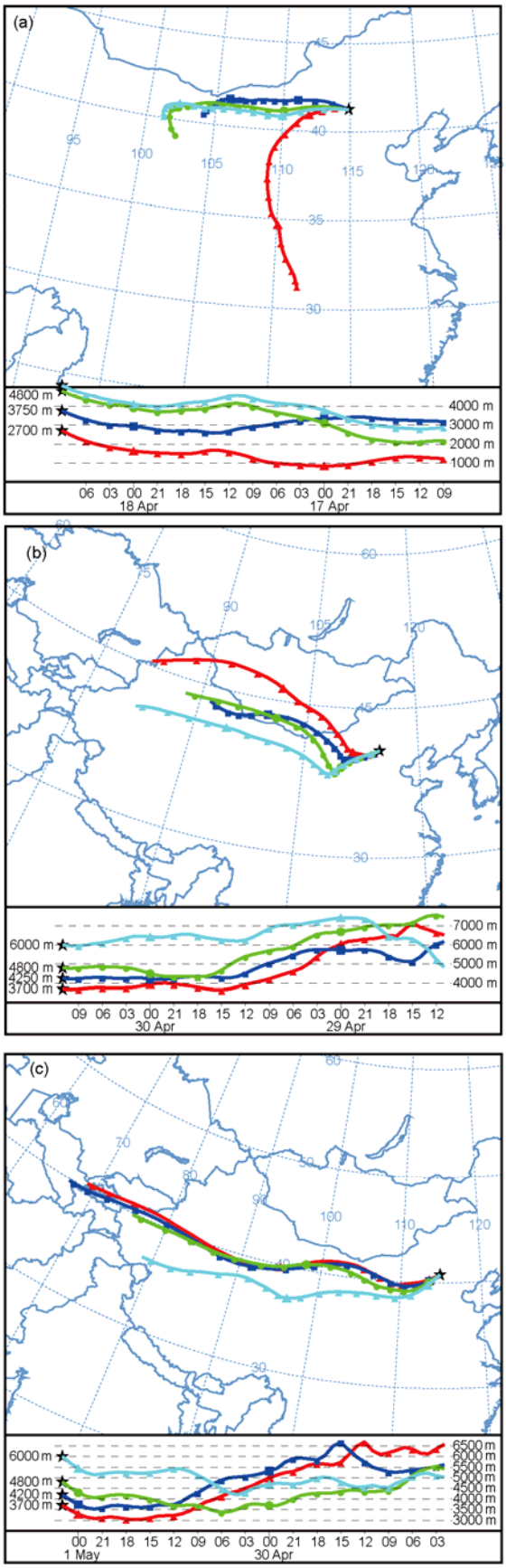

Figure 8 The 48-h back trajectories of air masses during the BCE. (a) 18 April; (b) 30 April; (c) 1 May.

3 Conclusions

The Beijing Cloud Experiment (BCE) of the Key Project in

the National Science & Technology Pillar Program during the Eleventh Five-year Plan Period is the first multi-aircraft cloud observational experiment in China. During this experiment, three aircrafts observed aerosol, CCN and cloud at different altitudes simultaneously, and provided valuable data for the aerosol-cloud interactions in this area. We analyzed the aerosol and CCN data of 18 April, 30 April and 1 May from this experiment and the results are summarized as follows:

(1) The results indicate that properties of the vertical distribution of aerosol number concentration were distinct under stable atmospheric stratification in spring in the study area. The aerosol number concentration could reach to the magnitude of 10^3 cm^{-3} below 4500 m and decreased to the magnitude of only 10 cm^{-3} as altitude increased above 4500 m.

(2) Aerosol mean diameters were between 0.16 and 0.19 μm, and changed little with altitude. Under influences of depletion of cloud and precipitation, evaporation, secondary aerosol and dust at high levels, the particle concentrations with diameter of 0.1 μm increased greatly at levels below 4500 m in 1 May, but the concentrations of particles with diameter ranging from 0.12 to 3 μm, especially from 0.16 to 0.3 μm, decreased distinctly. Aerosol mean diameters were between 0.11 and 0.12 μm. Above 4500 m, however, concentrations of particles with diameter ranging from 1.8 to 3 μm increased obviously.

(3) Below 4500 m, the average number size distributions of aerosol showed a bimodal (multimodal) mode, and unimodal mode above it.

(4) The vertical distribution of ratio of CCN concentration to aerosol number concentration suggests that the conversion ratios of aerosol to CCN at 0.3% supersaturation were less than 20% below 4500 m, and changed little with altitude. The ratios were between 12% and 15% in 18 and 30 April, and between 1.4% and 1.6% in 1 May. Above 4500 m, the conversion ratio increased with altitude and could reach as large as 50%. Moreover, the differences between days at the same level were distinct.

(5) The aerosol and CCN concentration data were fitted to establish a simple relationship between them. When excluded observations of 1 May, the correlation coefficients could reach 0.98 and decreased to 0.84 when included them.

(6) The different sources of aerosol made differences of aerosol number concentrations, size distributions and conversion ratios of aerosol to CCN between upper and lower levels. The back trajectories suggested that levels above 4500 m were influenced by large particles in these three days during the experiment. The high CCN to aerosol ratio (as large as 50%) suggested the high solubility of these large particles, and it had greater effect on cloud and precipitation under stable weather condition. Levels below 4500 m influenced more by local and surface pollutants, and the conversion rate of aerosol to CCN was as low as 20% although the pollution aerosol concentration was high. Under stable weather condition, these pollution aerosols only have small effect on cloud and precipitation because it was difficult to transport them to the upper levels.

Results above show that vertical distributions of aerosol and CCN and the magnitude of their concentrations during the BCE was consistent with Zhang et al. [22]. The aerosol number concentration decreased with altitude. The aerosol number concentrations in the BCE were much higher than that in the ACE-2 [43] and the INDOEX [44], but close to the continental aerosol observed at the Gulf of Mexico [45], and this is an important difference between continental and maritime aerosol, and suggesting that the observed area was heavily influenced by local pollution aerosols. Comparing with Zhang et al. [22], the conversion ratios of aerosol to CCN were much smaller, less than 15% at levels below 4500 m in the BCE and ranged from 30% to 50% in Zhang et al. [22]. Above 4500 m, the conversion ratios were close in these two experiments. It suggests that chemical compositions of aerosol below 4500 m in these two experiments were different. The possible cause is the difference of pollutant sources between these two regions when sampled. Levels above 4500 m were influenced less by pollutant that the difference of aerosol chemical property at these levels was smaller.

More accurate researches with CCN observations at much wider range of supersaturation are needed, because the CCN observed in the BCE was at 0.3% supersaturation, and this only told the story at a certain situation. Furthermore, aerosol chemical composition in this study was only an assumption because there was no chemical observation during the BCE. Whether the large particles at higher levels come from the dusts that interacted with pollution aerosols during transportation and formed the large soluble aerosols, or they were locally originate, needs further observations and verifications.

This work was supported by the Research and Development Special Fund for Public Welfare Industry (*Meteorology*) (*GYHY200806001*) *and the Key Project in the National Science & Technology Pillar Program* (*2006 BAC12B03*).

1 Twomey S. The influence of pollution on shortwave albedo of clouds. J Atmos Sci, 1977, 34: 1149–1152
2 Albrecht B A. Aerosols, cloud microphysics, and fractional cloudiness. Science, 1989, 245: 1227–1230
3 IPCC. Climate Change 2007: The Physical Science Basis. Cambridge: Cambridge University Press, 2007
4 Yum S S, Hudson J G. Maritime/continental microphysical contrasts in stratus. Tellus B-Chem Phys Meteorol, 2002, 54: 61–73
5 Hudson J G, Yum S S. Maritime/continental drizzle contrasts in small cumuli. J Atmos Sci, 2001, 58: 915–926
6 Hudson J G, Yum S S. Cloud condensation nuclei spectra and polluted and clean clouds over the Indian Ocean. J Geophys Res, 2002, 107, doi: 10.1029/2001JD000829
7 Bates T S, Huebert B J, Gras J L, et al. International Global Atmospheric Chemistry (IGAC) project's First Aerosol Characterization Experiment (ACE 1): Overview. J Geophys Res, 1998, 103: 16297–16318

8 Raes F, Bates T, McGovern F, et al. The 2nd Aerosol Characterization Experiment (ACE-2): General overview and main results. Tellus B-Chem Phys Meteorol, 2000, 52: 111–125
9 Huebert B J, Bates T, Russell P B, et al. An overview of ACE-Asia: Strategies for quantifying the relationships between Asian aerosols and their climatic impacts. J Geophys Res, 2003, 108, doi:10.1029/2003JD003550
10 Song K Y, Yum S S. Maritime-continental contrasts of cloud microphysics during ACE-Asia. J Korean Meteorol Soc, 2004, 40: 177–189
11 VanReken T M, Rissman T A, Roberts G C, et al. Toward aerosol/cloud condensation nuclei (CCN) closure during CRYSTAL-FACE. J Geophys Res, 2003, 108, doi: 10.1029/2003JD003582
12 Fan S, An X. Measurement and analysis of the concentration of cloud condensation nuclei in Mt. Helanshan area (in Chinese). J Desert Res, 2000, 20: 338–340
13 Niu S, Zhang C. Researches on sand aerosol chemical composition and enrichment factor in the spring at Helan Mountain area (in Chinese). J Desert Res, 2000, 20: 264–268
14 Niu S, Zhang C, Sun J. Observational researches on the size distribution of sand aerosol particles in the Helan Mountain area (in Chinese). Chin J Atmos Sci, 2001, 25: 243–252
15 Niu S, Sun J, Chen Y et al. Observation and analysis of mass concentration of dust and sand aerosol in spring in Helanshan area (in Chinese). Plateau Meteorol, 20: 82–87
16 Zhao Y, Niu S, Lü J, et al. Observational analyses on cloud condensation nuclei in northwestern China in summer of 2007 (in Chinese). Plateau Meteorol, 2010, 29: 1043–1049
17 Zhang D, Guo X, Fu D. Aircraft observation on cloud microphysics in Beijing and its surrounding regions during August–September 2003 (in Chinese). Chin J Atmos Sci, 31: 596–610
18 Fan Y, Guo X, Fu D, et al. Observational studies on aerosol distribution during August to September in 2004 over Beijing and its surrounding areas (in Chinese). Clim Environ Res, 2007, 12: 49–62
19 Shi L, Duan Y. Observations of cloud condensation nuclei in north China (in Chinese). Acta Meteorol Sin, 2007, 65: 644–652
20 Duan J, Mao J. Influence of aerosol on regional precipitation in North China. Chin Sci Bull, 2008, 54: 474–483
21 Zhang Q, Ma X, Tie X, et al. Vertical distributions of aerosols under different weather conditions: Analysis of *in-situ* aircraft measurements in Beijing, China. Atmos Environ, 2009, 43: 5526–5535
22 Zhang Q, Quan J, Tie X, et al. Impact of aerosol particles on cloud formation: Aircraft measurements in China. Atmos Environ, 2011, 45: 665–672
23 Ning D T, Zhong L X, Chung Y S. Aerosol size distribution and elemental composition in urban areas of Northern China. Atmos Environ, 1996, 30: 2355–2362
24 Zhang R, Wang M, Fu J. Preliminary research on the size distribution of aerosols in Beijing. Adv Atmos Sci, 2001, 18: 225–230
25 Guinot B, Roger J C, Cachier H, et al. Impact of vertical structure on Beijing aerosol distribution. Atmos Environ, 2006, 40: 5167–5180
26 Wu Z, Hu M, Liu S, et al. New particle formation in Beijing, China: Statistical analysis of a 1-year data set. J Geophys Res, 2007, 112, doi: 10.1029/2006JD007406
27 Liu S, Hu M, Wu Z, et al. Aerosol number size distribution and new particle formation at a rural/coastal site in Pearl River Delta (PRD) of China. Atmos Environ, 2008, 42: 6275–6283
28 Qian Y, Gong D, Fan J, et al. Heavy pollution suppresses light rain in China: Observations and modeling. J Geophys Res, 2009, 114, doi: 10.1029/2008JD011575
29 Rose D, Nowak A, Achtert P, et al. Cloud condensation nuclei in polluted air and biomass burning smoke near the mega-city Guangzhou, China—Part 1: Size-resolved measurements and implications for the modeling of aerosol particle hygroscopicity and CCN activity. Atmos Chem Phys, 2010, 10: 3365–3383
30 Rose D, Gunthe S S, Su H, et al. Cloud condensation nuclei in polluted air and biomass burning smoke near the mega-city Guangzhou, China—Part 2: Size-resolved aerosol chemical composition, diurnal cycles, and externally mixed weakly CCN-active soot particles. Atmos Chem Phys, 2011, 11: 2817–2836
31 Yu X, Zhu B, Yin Y, et al. A comparative analysis of aerosol properties in dust and haze-fog days in a Chinese urban region. Atmos Res, 2011, 99: 241–247
32 Deng Z Z, Zhao C S, Ma N, et al. Size-resolved and bulk activation properties of aerosols in the North China Plain. Atmos Chem Phys, 2011, 11: 3835–3846
33 Shen X J, Sun J Y, Zhang Y M, et al. First long-term study of particle number size distributions and new particle formation events of regional aerosol in the North China Plain. Atmos Chem Phys, 2011, 11: 1565–1580
34 Rose D, Gunthe S S, Mikhailov E, et al. Calibration and measurement uncertainties of a continuous-flow cloud condensation nuclei counter (DMT-CCNC): CCN activation of ammonium sulfate and sodium chloride aerosol particles in theory and experiment. Atmos Chem Phys, 2008, 8: 1153–1179
35 Gultepe I, Isaac G A, Leaitch W R, et al. Parameterization of marine stratus of microphysics based on *in situ* observations: Implications for GCMS. J Clim, 1996, 9: 345–357
36 Gultepe I, Isaac G A. Aircraft observations of cloud droplet number concentration: Implications for climate studies. Quart J Roy Meteor Soc, 2004, 130: 2377–2390
37 Hobbs P V, Rangno A L. Microstructures of low and middle-level clouds over the Beaufort Sea. Quart J Roy Meteor Soc, 1998, 124: 2035–2071
38 Rangno A L, Hobbs P V. Microstructures and precipitation development in cumulus and small cumulonimbus clouds over the warm pool of the tropical Pacific Ocean. Quart J Roy Meteor Soc, 2005, 131: 639–673
39 Stith J L, Haggerty J, Grainger C, et al. A comparison of the microphysical and kinematic characteristics of mid-latitude and tropical convective updrafts and downdrafts. Atmos Res, 2006, 82: 350–366
40 Peter J R, Siems S T, Jensen J B, et al. Airborne observations of the effect of a cold front on the aerosol particle size distribution and new particle formation. Quart J Roy Meteor Soc, 2010, 136: 944–961
41 Dusek U, Frank G P, Hildebrandt L, et al. Size matters more than chemistry for cloud nucleating ability of aerosol particles. Science, 2006, 312: 1375–1378
42 Draxler R R, Hess G D. An overview of the HYSPLIT_4 modelling system for trajectories, dispersion, and deposition. Aust Met Mag, 1998, 47: 295–308
43 Chuang P Y, Collins D R, Pawlowska H, et al. CCN measurements during ACE-2 and their relationship to cloud microphysical properties. Tellus B-Chem Phys Meteorol, 2000, 52: 843–867
44 Ramanathan V, Crutzen P J, Lelieveld J, et al. Indian Ocean experiment: an integrated analysis of the climate forcing and effects of the great Indo-Asian haze. J Geophys Res, 2001, 106: 28371–28399
45 Lu M L, Feingold G, Jonsson H H, et al. Aerosol-cloud relationships in continental shallow cumulus. J Geophys Res, 2008, 113, doi: 10.1029/2007JD009354